Original article

Nuclear Medicine Communications

Comparison of ^{18}F-FDG PET/CT and ^{68}Ga-FAPI-04 PET/CT in patients with non-small cell lung cancer

Canan Can[a], Ferat Kepenek[a], Halil Kömek[a], Cihan Gündoğan[a], İhsan Kaplan[a], Bekir Taşdemir[b], Yunus Güzel[a], Nurşin Agüloğlu[c] and Hüseyin Karaoğlan[a]

Aim **In this study, we aimed to compare the diagnostic accuracy of ^{18}F–fluorodeoxyglucose (^{18}F-FDG) and Gallium-68 labeled fibroblast activator protein inhibitor (^{68}Ga-FAPI)-04 PET/CT in the tumor–node–metastasis (TNM) staging of patients with nonsmall cell lung cancer (NSCLC) and investigate whether adenocarcinoma (ADC) and squamous cell cancer (SCC) exhibit different uptake patterns on ^{68}Ga-FAPI-04 PET/CT.**

Materials and method **Twenty-nine patients with a histopathologically-confirmed diagnosis of NSCLC, who had no history of previous radiation therapy or chemotherapy and underwent ^{18}F-FDG PET/CT and ^{68}Ga-FAPI-04 PET/CT imaging between January 2021 and December 2021 were included in this retrospective study. Staging was performed using the 8th edition of the TNM staging system on both ^{18}F-FDG PET/CT and ^{68}Ga-FAPI-04 PET/CT images. Standardized uptake value $(SUV)_{max}$ and tumor-to-background ratios (TBR) were calculated on primary lesions and metastases.**

Results **There was no statistically significant difference in primary lesions in terms of SUV_{max} and TBR values. However, ^{68}Ga-FAPI-04 PET/CT was significantly superior to ^{18}F-FDG PET/CT in terms of the number of lymph nodes and bone metastases revealed. The SUV_{max} and TBR values of lymph nodes, hepatic lesions and bone lesions were significantly higher on ^{68}Ga-FAPI-04 PET/CT than on ^{18}F-FDG PET/CT. ^{68}Ga-FAPI-04 PET/CT changed the disease stage of three patients (10.9%). The diagnostic accuracy of ^{68}Ga-FAPI-04 PET/CT was 100%, whereas the diagnostic accuracy of ^{18}F-FDG PET/CT was 89.6% (P=0.250).**

Conclusion **Although ^{68}Ga-FAPI-04 PET/CT detected more lesions and higher diagnostic accuracy than ^{18}F-FDG PET/CT in NSCLC, neither method was statistically superior to each other in terms of diagnostic accuracy in TNM staging. *Nucl Med Commun* XXX: 000–000**

Nuclear Medicine Communications XXX, **XXX**:000–000

Keywords: ^{18}**F- FDG,** ^{68}**Ga-FAPI-04, NSCLC, PET/CT,** SUV_{max}

[a]Department of Nuclear Medicine, Gazi Yasargil Training and Research Hospital, [b]Department of Nuclear Medicine, Dicle University Faculty of Medicine, Diyarbakır and [c]Department of Nuclear Medicine, Saglik Bilimleri University Dr. Suat Seren Chest Diseases and Surgery Hospital, İzmir, Turkey

Correspondence to Halil Kömek, MD, Department of Nuclear Medicine, Gazi Yasargil Training and Research Hospital, 21070, Kayapınar, Diyarbakir, Turkey
Tel: +904122580101; e-mail: halilkomek@gmail.com

Received 1 June 2022 **Accepted** 18 July 2022

Introduction

According to the Global Cancer Statistics 2020 data, lung cancer is the second most diagnosed type of cancer worldwide (11.4%) and is the leading cause of cancer-related deaths (18%) [1]. Non-small cell lung cancer (NSCLC) accounts for approximately 85% of all lung cancer cases [2]. Accurate staging of NSCLC has major importance in the patient management, especially in deciding the optimal treatment strategy and predicting prognosis. ^{18}F–fluorodeoxyglucose (^{18}F-FDG) is widely accepted as a noninvasive technique for lung cancer staging in various international guidelines [3]. ^{18}F-FDG PET/CT can provide more accurate staging than conventional imaging methods and helps avoiding unnecessary surgical interventions [4].

Gallium-68 labeled fibroblast activator protein inhibitor (^{68}Ga-FAPI) is a novel PET tracer agent. Due to its low physiologic uptake in the liver, bones and gastrointestinal system as well as high tumor-to-background ratio (TBR), ^{68}Ga-FAPI PET/CT is reported to be superior to ^{18}F-FDG PET/CT in various tumors [5–7].

In this study, we aimed to compare the diagnostic accuracy of ^{18}F-FDG PET/CT and ^{68}Ga-FAPI-04 PET/CT in the tumor–node–metastasis (TNM) staging of patients with nonsmall cell lung cancer (NSCLC) and investigate whether adenocarcinoma (ADC) and squamous cell cancer (SCC) exhibit different uptake patterns on ^{68}Ga-FAPI-04 PET/CT.

Materials and method

Patient selection

Twenty-nine patients with a histopathologically-confirmed diagnosis of NSCLC, who underwent ^{18}F-FDG PET/CT and ^{68}Ga-FAPI-04 PET/CT imaging between January 2021 and December 2021, were included in this retrospective study. This study was designed

0143-3636 DOI: 10.1097/MNM.0000000000001607

retrospectively from an unpublished prospective study comparing ^{18}F-FDG PET/CT and ^{68}Ga-FAPI-04 PET/CT in the differential diagnosis of benign and malignant thoracic lesions. (approval no:721). Patients who were older than 18 years, had a histopathologically-confirmed diagnosis of NSCLC, had an Eastern Clinical Oncology Group performance score of 0–2, had no previous history of radiation therapy or chemotherapy and had the imaging scans performed maximum 2 weeks (1–14 days) apart were included in the study. Patients with severe hepatic or renal failure, who could not be screened, who had secondary malignancies and who could not be followed up were excluded from the study. Fifteen of the patients had received a diagnosis before the scans, and histopathologic evaluation of the remaining 14 patients was completed after the scans. In hepatic, bone and lymph node metastases, histopathological correlation was made from target lesions and pathology reports were recorded. For lesions that are not biopsied; lesions with confirmed metastases on CT, MRI and imaging performed after at least 3 months of follow-up were considered positive. All patients underwent hepatic and cranial MRI. This study was conducted in concordance with the current law and good clinical practice guidelines. Approval from the local ethics committee was obtained (approval no: 2021/955). All patients or their relatives provided verbal and written informed consent.

PET/CT protocol and image analysis

All patients were asked to fast for at least 6 h before ^{18}F-FDG imaging. Blood glucose was confirmed to be ≤140 mg/dL using the fingerstick method, and 3.5–5.5 MBq/kg of FDG was intravenously injected. Fasting and blood glucose measurements were not required for ^{68}Ga-FAPI PET/CT imaging, and the radiotracer was injected at a dose of 2 Mbq/kg. All images were obtained using Discovery IQ 4 ring 20 cm axial field-of-view (FOV) PET/CT (GE Healthcare, Milwaukee, Wisconsin, USA). After the injection, whole-body ^{68}Ga-FAPI-04 PET/CT and ^{18}F-FDG FDG PET/CT images were obtained from the vertex to the middle of the thigh at 55–65 min. After CT images (CT parameters: 120 kV, 80 mAs/slice, 700 mm transaxial FOV, no gap, 64 × 0.625 mm collimation, pitch 1.4, 0.5 s rotation time, 3.3 mm slice thickness, 512 × 512 matrix), PET images [PET parameters: 3D FOV 20 cm, ordered subset expectation–maximization algorithm (OSEM) 5 iterations/12 subsets, fullwidth at half maximum (FWHM) 3 mm) were taken at the bedside at 2.5 min in the same position to include the same regions. All ^{68}Ga-FAPI-04 PET/CT and ^{18}F-FDG FDG PET/CT images were reviewed on AW 4.7 (Advantage Workstation software version 4.7 GE Healthcare) by two specialists with at least 10 years of PET/CT experience. After excluding physiological uptake sites, increased uptake above the background level was accepted as positive. Primary tumor and metastatic lesions were counted on ^{18}F-FDG and ^{68}Ga-FAPI PET/CT images. Standardized uptake value $(SUV)_{max}$ values were calculated by drawing volumes of interest (VOIs) from the primary tumor and metastatic lesions. Background values were obtained by drawing VOIs from the tumor-free lung parenchyma, descending thoracic aorta, liver and L2 vertebra (from another lumbar vertebra in the presence of metastasis). TBR were calculated by dividing the SUV_{max} values obtained from primary tumors and metastases to background values. The staging was performed using the 8th edition of the TNM staging system on both ^{18}F-FDG PET/CT and ^{68}Ga-FAPI-04 PET/CT images.

Statistical analysis

SPSS version 25.0 (IBM Corporation, Armonk, New York, USA) software was used for statistical analyses. A comparison of two dependent and non-normally distributed variables was performed using Wilcoxon's signed rank test. The diagnostic accuracies of ^{18}F-FDG and ^{68}Ga-FAPI PET/CT were compared with the McNemar test. A comparison of TNM score compatibility between groups was performed with Cohen's Kappa analysis. Mann–Whitney U test was preferred for the comparison of adenocarcinoma and SCC groups. $P < 0.05$ was considered statistically significant.

Results

Among the 29 patients included in our study, 27 (93.1%) were male. The median age was 71 years (46–84). Twenty patients (69%) had SCC, whereas 9 (31%) had adenocarcinoma. All primary lesions exhibited radiotracer uptake on ^{68}Ga-FAPI PET/CT and ^{18}F-FDG PET/CT (Fig. 1). ^{18}F-FDG PET/CT revealed 145 lymph nodes in 21 patients, whereas ^{68}Ga-FAPI PET/CT showed 160 lymph nodes in 20 patients ($P = 0.002$). The mediastinal lymph nodes of two patients that showed increased uptake on ^{18}F-FDG PET/CT but no uptake on ^{68}Ga-FAPI PET/CT were found to have benign pathology after mediastinoscopic biopsy (Fig. 2). Histopathologic evaluation of one mediastinal lymph node of one patient with no ^{18}F-FDG uptake but increased ^{68}Ga-FAPI uptake showed metastasis. ^{18}F-FDG PET/CT revealed 11 pleural lesions in six patients, whereas ^{68}Ga-FAPI PET/CT showed 15 pleural lesions with increased uptake in eight patients, one of which had diffuse uptake ($P = 0.046$) (Fig. 3). In 11 patients with bone metastases, 109 bone lesions were visualized on ^{18}F-FDG PET/CT, whereas 135 bone lesions were seen on ^{68}Ga-FAPI PET/CT ($P < 0.001$). Brain metastasis observed in one patient with 68Ga-FAPI PET/CT was not observed with 18F-FDG PET/CT. No statistically significant difference was observed between the two imaging methods in terms of lesion detection in hepatic, pulmonary and adrenal metastases (Table 1).

There was no statistically significant difference in primary lesions in terms of SUV_{max} and TBR values measured on the two imaging methods ($P = 0.339$ and 0.133,

Fig. 1

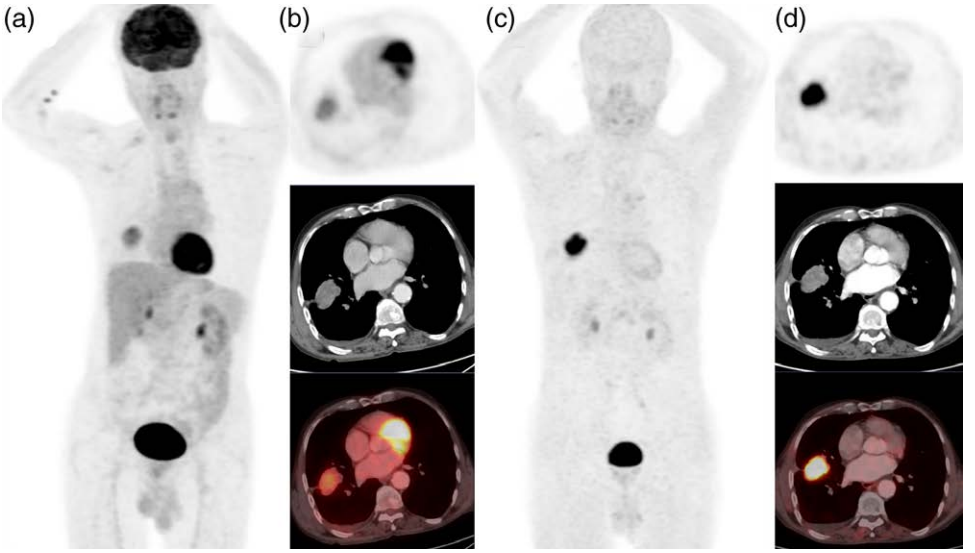

Patient no:6. The primary tumor SUV_{max} was 7 on ^{18}F-FDG PET/CT (a: MIP, b: Axial PET-CT-Fusion images) and 15.8 on ^{68}Ga-FAPI-04 PET/CT (c: MIP, d: Axial PET-CT-Fusion images). Pleural effusion observed in both scans was histopathologically benign. ^{18}FFDG, ^{18}F—fluorodeoxyglucose; SUV, standardized uptake value.

Fig. 2

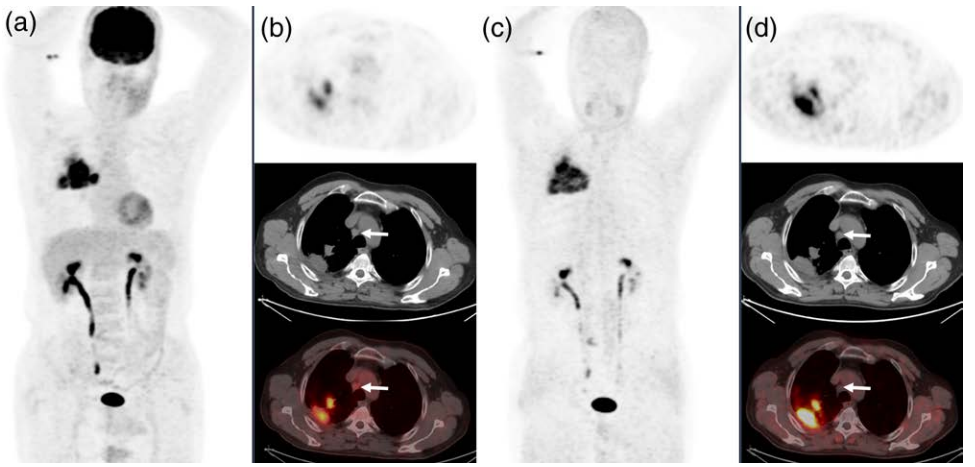

Patient no:29. The primary tumor SUV_{max} was 18.3 on ^{18}F-FDG PET/CT (a: MIP, b: Axial PET-CT-Fusion images) and 19 on ^{68}Ga-FAPI-04 PET/CT (c: MIP, d: Axial PET-CT-Fusion images). The SUV_{max} of the right paratracheal lymph node (arrows) observed on ^{18}F-FDG PET/CT, which was found to be benign after mediastinoscopic biopsy, was 2.4, and no uptake was observed in ^{68}Ga-FAPI-04 PET/CT. Mediastinal background SUV_{max} was 1.7 on ^{18}F-FDG PET/CT. ^{18}FFDG, ^{18}F—fluorodeoxyglucose; SUV, standardized uptake value.

respectively). The SUV_{max} and TBR values of lymph nodes (Fig. 4), hepatic lesions and bone lesions (Fig. 5) were significantly higher on ^{68}Ga-FAPI-04 PET/CT than on ^{18}F-FDG PET/CT ($P<0.001$ for all). No statistically significant difference was found in the SUV_{max} and TBR values of pulmonary and pleural metastases with both imaging methods ($P>0.005$) (Table 2).

According to the TNM stage; 28 patients showed compatible T stage with both FDG and FAPI PET/CT. One patient with T2 disease on ^{18}F-FDG PET/BT was evaluated as T4 on ^{68}Ga-FAPI-04 PET/CT because the nodule in a different lobe showed FAPI uptake. The kappa coefficient of the two methods was 0.949, and the diagnostic accuracies of ^{68}Ga-FAPI PET/CT and ^{18}F-FDG PET/CT for determining the T stage were 100 and 96.5%, respectively ($P>0.05$). Twenty-five patients had compatible N stage with both FDG and FAPI PET/CT (k: 0.806). The diagnostic accuracy of ^{68}Ga-FAPI-04 PET/CT in

Fig. 3

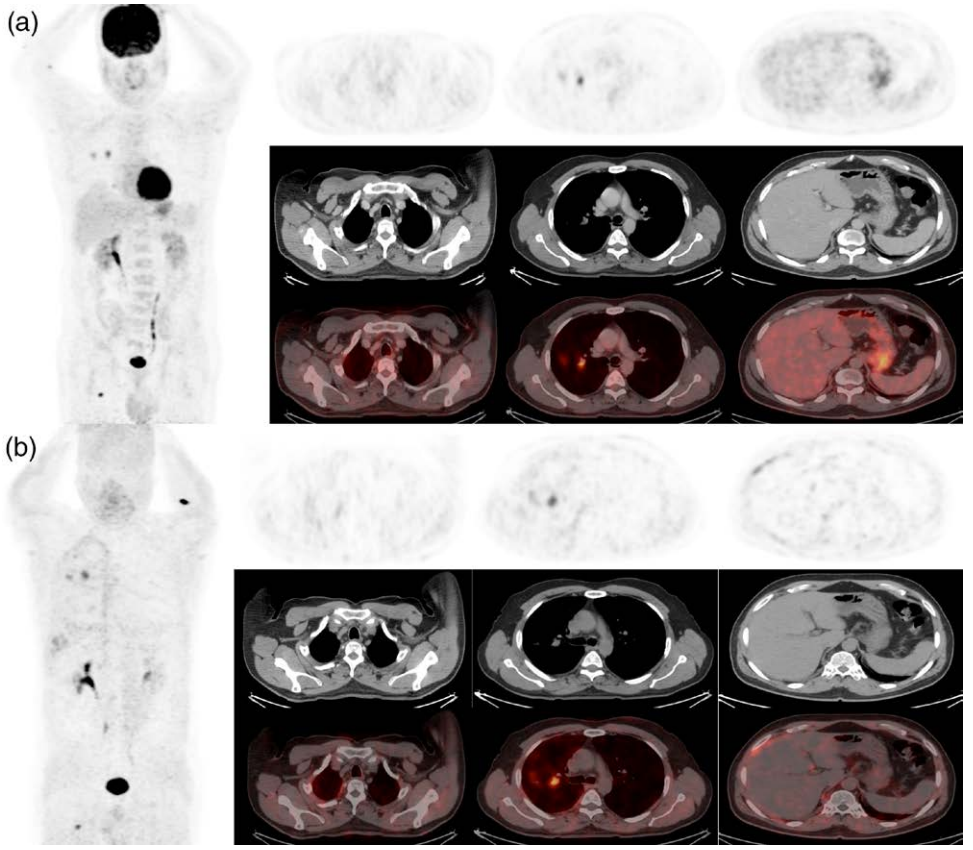

Patient no:1. The primary tumor SUV_{max} was 6.9 on ^{18}F-FDG PET/CT (a: MIP, Axial PET-CT-Fusion images) and 7.2 on ^{68}Ga-FAPI-04 PET/CT. ^{68}Ga-FAPI-04 PET/CT (b: MIP, Axial PET-CT-Fusion images). showed increased pleural uptake with a 4.3 SUV_{max}, while there was no FDG uptake in this area. Pleural biopsy revealed adenocarcinoma infiltration. ^{18}FFDG, ^{18}F—fluorodeoxyglucose; standardized uptake value.

determining the N stage was 100%, whereas this rate was 86.2% for ^{18}F-FDG PET/CT ($P=0.125$). ^{68}Ga-FAPI-04 PET/CT changed the N stage of four patients (13.9%). Twenty-eight patients showed compatible M stage with both FDG and FAPI PET/CT (k: 0.947). The diagnostic accuracy of ^{68}Ga-FAPI-04 PET/CT in determining the M stage was 100%, whereas this rate was 95.6% for ^{18}F-FDG PET/CT ($P>0.05$). ^{68}Ga-FAPI-04 PET/CT changed the M stage of one patient (3.4%) who had pleural involvement (M0 to M1a). Twenty-six patients had compatible disease stage with both FDG and FAPI PET/CT (k: 0.868). ^{68}Ga-FAPI-04 PET/CT changed the disease stage of 3 (10.9%) patients (2 downstage and 1 upstage). The diagnostic accuracy of ^{68}Ga-FAPI-04 PET/CT was 100%, whereas the diagnostic accuracy of ^{18}F-FDG PET/CT was 89.6% ($P=0.250$). Although ^{68}Ga-FAPI-04 PET/CT showed higher diagnostic accuracy in T, N and M staging and stage, neither method was found to be statistically superior to the other. (Table 3). TNM staging of all patients with ^{18}F-FDG PET/CT and ^{68}Ga-FAPI PET/CT are presented in Table 4.

Age, primary tumor FDG SUV_{max}, and primary tumor FDG TBR values were significantly higher in patients with SCC than in adenocarcinoma ($P=0.047$, 0.012 and 0.048, respectively). There was no significant difference in the SUV_{max} and TBR values of primary lesions with adenocarcinoma and SCC pathology on ^{68}Ga-FAPI-04 PET/CT. However, TBR values of the bone metastases were observed to be higher in the SCC group than in the adenocarcinoma group ($P=0.023$). The adenocarcinoma and SCC groups exhibited no statistically significant difference in terms of other parameters (Table 5).

Discussion

In this retrospective study with NSCLC patients, ^{68}Ga-FAPI PET/CT changed the disease stage and is found to be superior to ^{18}F-FDG PET/CT in TNM staging.

NSCLC includes a heterogenous group of carcinomas with varying tumor biology and prognosis [8]. National Comprehensive Cancer Network guidelines recommend ^{18}F-FDG PET/CT for the evaluation of patients with NSCLC of all stages [9]. Recently, promising studies

have been conducted in the staging of lung cancer with FAPI-labeled radiotracers [10–12].

In the current study, consistent with previous studies [10,13,14], ^{18}F-FDG and ^{68}Ga-FAPI PET/CT were found to be similar in detecting the primary tumor, and no statistically significant difference was observed in terms of SUV_{max} and TBR values. However, in a recent study by Wang *et al.* [11] the researchers reported significantly higher primary tumor SUV_{max} on ^{68}Ga-FAPI PET/CT than ^{18}F-FDG PET/CT. Our median SUV_{max} was >12, which was also in concordance with the previous literature [6,12]. One patient in our series was upstaged in T staging with ^{68}Ga-FAPI PET/CT due to a pulmonary nodule in a different lobe that showed no FDG uptake but increased FAPI uptake.

Table 1 Comparison of descriptive parameters and number of lesions between ^{18}F-FDG PET/CT and ^{68}Ga-FAPI-04 PET/CT

	N	Mean ± std	Median	Min-max
Primary lesion size(mm)	29	57.7 ± 24.4	55	9.8–103
Age	29	67.0 ± 9.6	71	46–85
		N	%	
Sex	Female	2	6.9	
	Male	27	93.1	
Tumor subtype	ADC	9	31	
	SCC	20	69	
Tumor location	Right	13	44.8	
	Left	16	55.2	
		NP	NL	P[a]
Primary tumor	FDG	29	29	Ns
	FAPI	29	29	
Lymph node metastasis	FDG	21	145	0.002
	FAPI	20	160	
Bone metastasis	FDG	11	109	<0.001
	FAPI	11	135	
Liver metastasis	FDG	7	18	0.317
	FAPI	7	19	
Lung metastasis	FDG	6	17	0.157
	FAPI	7	19	
Pleural metastasis	FDG	6	11	0.46
	FAPI	8	15	
Adrenal metastasis	FDG	3	5	1.00
	FAPI	3	5	
Brain metastasis	FDG	0	0	Ns
	FAPI	1	1	

ADC, adenocarcinoma; FAPI, fibroblast activator protein inhibitor; 18FFDG, 18F–fluorodeoxyglucose; min, minimum; max, maximum; NL, number of lesion; NP, number of patient; Ns, non significant; SCC, squamous cell cancer.
[a]Wilcoxon signed-rank test.

In a meta-analysis of patients with NSCLC, the sensitivity and specificity of ^{18}F-FDG PET/CT were reported to be 72 and 91%, respectively [15]. In the current study, a higher number of positive lymph nodes were visualized on ^{68}Ga-FAPI PET/CT, and the diagnostic accuracy of FAPI PET/CT, SUV_{max} and TBR values were significantly higher than ^{18}F-FDG PET/CT. Similarly, previous studies have also found ^{68}Ga-FAPI PET/CT superior in terms of detecting lymph nodes and SUV_{max} [10,13]. ^{18}F-FDG PET/CT can have false positive results in sarcoidosis, tuberculosis, pneumonia, silicosis and emphysema [16–18]. In our study, mediastinal lymph nodes of two patients that were false positive on ^{18}F-FDG PET/CT due to anthracosis were negative on ^{68}Ga-FAPI PET/CT. Similar recent case reports support our findings [19,20]. Lymph node parameters less than 10 mm, low metabolic activity and small tumor volume can cause false negativity on ^{18}F-FDG PET/CT [18,21]. In our study, an 11 mm paratracheal lymph node of a patient with no uptake on ^{18}F-FDG PET/CT exhibited tracer uptake on ^{68}Ga-FAPI PET/CT and histopathologic evaluation revealed lymph node metastasis. In their study, Li *et al.* [10] observed a change in N stage in 11.8% of patients with FAPI, whereas we observed a change in N stage in 13.9% of patients.

^{18}F-FDG PET/CT is superior to other imaging techniques in M staging of lung cancer, except for brain metastases [15,22,23]. Studies comparing FAPI PET/

Fig. 4

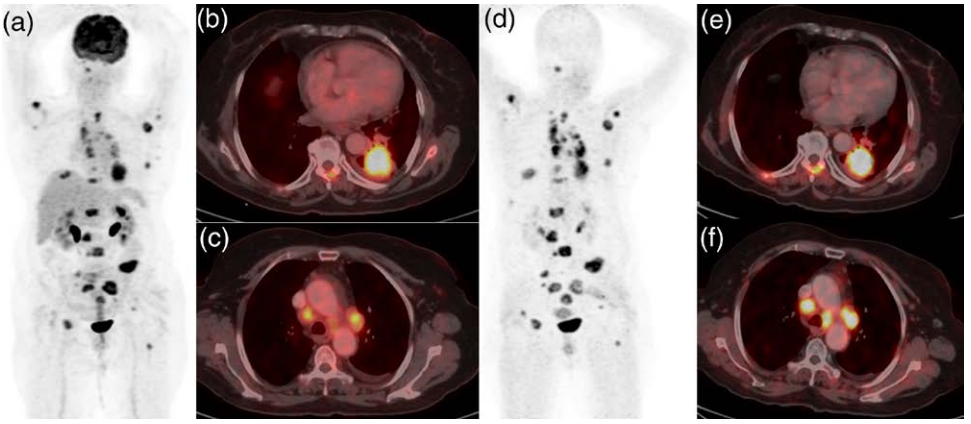

Patient no:7. The primary tumor SUV_{max} was 13.6 on ^{18}F-FDG PET/CT (a: MIP, b: Axial PET-CT-Fusion images) and 21.3 on ^{68}Ga-FAPI-04 PET/CT (c: MIP, d: Axial PET-CT-Fusion images). The SUV_{max} of mediastinal lymph nodes was 9.8 and 21.6, respectively. Higher SUV_{max} and TBR values were observed on ^{68}Ga-FAPI-04 PET/CT. ^{18}FFDG, ^{18}F—fluorodeoxyglucose; SUV, standardized uptake value.

Fig. 5

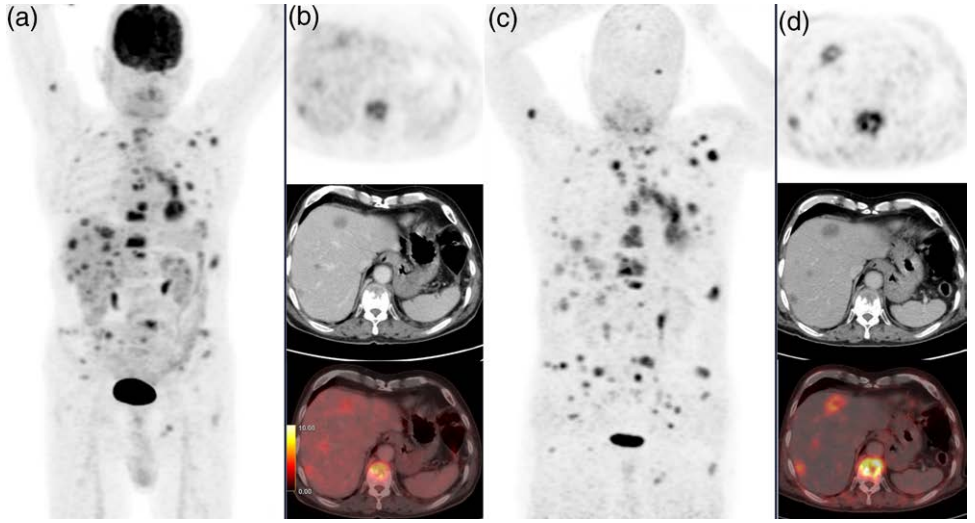

Patient no:4. The primary tumor SUV_{max} was 7.4 on ^{18}F-FDG PET/CT (a: MIP, b: Axial PET-CT-Fusion images) and 10 on ^{68}Ga-FAPI-04 PET/CT (c: MIP, d: Axial PET-CT-Fusion images). The SUV_{max} of metastatic hepatic lesions were 4 and 5.4 on ^{18}F-FDG PET/CT and ^{68}Ga-FAPI-04 PET/CT, respectively, while the TBR values were 1.81 and 4.9, respectively. The SUV_{max} of vertebra were 9.3 and 15.1 on ^{18}F-FDG PET/CT and ^{68}Ga-FAPI-04 PET/CT, respectively, while the TBR values were 4.22 and 25.16, respectively. ^{18}FFDG, ^{18}F–fluorodeoxyglucose; SUV, standardized uptake value.

Table 2 Comparison of SUV_{max} and tumor-to-background ratios of ^{18}F-FDG PET/CT and^{68}Ga-FAPI-04 PET/CT

	N	Mean±std	Median	Min-max	*P*
Primary tumor size (mm)	29	57.68±24.43	55.00	9.8–103.0	
Primary tumor FDG SUV_{max}	29	15.16±8.03	13.50	1.33–32.6	0.339
Primary tumor FAPI SUV_{max}	29	13.30±6.08	13.30	0.7–25.8	
Primary tumor FDG TBR	29	29.40±21.49	19.13	5.32–95.88	0.133
Primary tumor FAPI TBR	29	22.18±12.00	20.88	1.89–50.59	
Lymph node size (mm)	145	12.75±6.14	11.00	4–36	
Lymph node FDG SUV_{max}	154	7.84±3.69	7.40	1.8–19.1	<0.001
Lymph node FAPI SUV_{max}	160	11.91±5.60	11.20	1.6–28	
Lymph node FDG TBR	146	3.90±2.15	3.67	0.94–12.82	<0.001
Lymph node FAPI TBR	160	6.52±3.24	6.47	0.84–18.75	
Bone metastases FDG SUV_{max}	109	7.59±4.87	6.05	2.4–25.1	<0.001
Bone metastases FAPI SUV_{max}	135	10.97±6.32	9.50	2.7–33.3	
Bone metastases FDG TBR	118	3.16±3.09	2.27	0.71–20.92	<0.001
Bone metastases FAPI TBR	135	15.93±8.95	14.43	2.33–46.80	
Liver metastases size (mm)	10	19.00±12.97	13.50	8–45	
Liver metastases FDG SUV_{max}	18	6.55±3.35	5.55	3.8–16	<0.001
Liver metastases FAPI SUV_{max}	19	6.51±2.80	6.10	2.8–14.2	
Liver metastases FDG TBR	18	2.47±0.87	2.36	1.30–4.57	<0.001
Liver metastases FAPI TBR	19	6.05±3.46	5.40	0.97–15.78	
Lung metastases size (mm)	17	10.33±3.96	10.00	5–20	
Lung metastases FDG SUV_{max}	17	4.64±3.26	4.10	0.9–12.7	0.184
Lung metastases FAPI SUV_{max}	19	3.85±2.56	3.30	0.9–7.6	
Lung metastases FDG TBR	17	9.00±7.50	5.65	1.25–26.46	0.227
Lung metastases FAP TBRI	19	7.94±5.85	7.06	1.82–22.35	
Pleural metastases FDG SUV_{max}	11	4.45±4.41	3.10	2–17	0.168
Pleural metastases FAPI SUV_{max}	15	5.27±2.25	4.90	2–8	
Adrenal metastases size (mm)	5	26.8±11	23	17–44	
Adrenal metastases FDG SUV_{max}	5	10.38±6.32	9.5	2.7–19.3	0.080
Adrenal metastases FAPI SUV_{max}	5	7.36±3.30	7.7	3.8–12.2	

FAPI, fibroblast activator protein inhibitor; ^{18}FFDG, ^{18}F–fluorodeoxyglucose; max, maximum; min, minimum; SUV, standardized uptake value; TBR, tumor-to-background ratios.
[a]Wilcoxon Signed Ranks Test.

CT and ^{18}F-FDG PET/CT reported more metastases and higher SUV and TBR values with FAPI PET/CT [10,11,18]. In the current study, we observed more metastatic lesions in bones, pleura, brain, liver and lungs on FAPI PET/CT and the SUV_{max} and TBR values of bone and hepatic metastases were found to be higher than ^{18}F-FDG PET/CT. No statistically significant difference was found between the two imaging methods in

Table 3 The diagnostic accuracy of ^{18}F-FDG PET/CT and ^{68}Ga-FAPI-04 PET/CT in TNM staging and kappa correlation coefficients

	T staging FDG vs. FAPI			N staging FDG vs. FAPI			M staging FDG vs. FAPI			Stage FDG vs. FAPI		
	ACC %	P^a	K	ACC %	P^a	K	ACC %	P^a	K	ACC %	P^a	K
FDG	96.5	1.00	0.949	89.6	0.125	0.855	95.6	1.00	0.947	89.6	0.250	0.868
FAPI	100			95.6			100			100		

ACC, diagnostic accuracy; FAPI, fibroblast activator protein inhibitor; ^{18}FFDG, ^{18}F–fluorodeoxyglucose; K, Cohen's Kappa coefficient; TNM, tumor–node–metastasis.
[a]McNemar test.

Table 4 TNM staging of all patients with ^{18}F-FDG PET/CT and ^{68}Ga-FAPI-04 PET/CT

Patient no	Sex	Age	Tumor subtype	Tumor location	Primary tumor size	TNM stage FDG	TNM stage FAPI	True TNM	Stage FDG	Stage FAPI	True stage
1	E	47	ADC	Right	57	T3N0M1b	T3N0M1b	T3N0M1b	4A	4A	4A
2	E	58	ADC	Right	43	T4N2M1c	T4N2M1c	T4N2M1c	4B	4B	4B
3	E	57	ADC	Left	23	T1cN2M0	T1c N2M0	T1c N2M0	3B	3A	3A
4	E	72	ADC	Left	102	T4N2M1c	T4N3M1c	T4N3M1c	4B	4B	4B
5	E	69	ADC	Left	9.8	T1aN3M1b	T1aN3M1b	T1aN3M1b	4A	4A	4A
6	E	71	ADC	Right	48	T2bN0M0	T2bN0M0	T2bN0M0	2A	2A	2A
7	K	71	ADC	Left	38	T2bN3M1c	T2bN3M1c	T2bN3M1c	4B	4B	4B
8	E	58	ADC	Left	70	T4N2M0	T4N2M0	T4N2M0	3B	3B	3B
9	E	55	ADC	Right	26	T1cNOM1c	T1c N2M1c	T1c N2M1c	4B	4B[a]	4B
10	E	71	SCC	Left	80	T4N3M1c	T4N3M1c	T4N3M1c	4B	4B	4B
11	E	70	SCC	Left	66	T4N3M1c	T4N3M1c	T4N3M1c	4B	4B	4B
12	E	74	SCC	Right	48	T4N3M1a	T4N3M1a	T4N3M1a	4A	4A	4A
13	E	84	SCC	Left	78	T4N1M0	T4N1M0	T4N1M0	3A	3A	3A
14	E	75	SCC	Right	72	T4N1M0	T4N1M1a	T4N1M1a	3A	4A[b]	4A
15	K	46	SCC	Left	53	T3N1M0	T3N0M0	T3N0M0	3A	2B[c]	2B
16	E	79	SCC	Left	72	T4N2M1c	T4N2M1a	T4N2M1a	4B	4B	4B
17	E	65	SCC	Left	98	T4N0M0	T4N0M0	T4N0M0	3A	3A	3A
18	E	71	SCC	Left	68	T3N0M0	T3N0M0	T3N0M0	2B	2B	2B
19	E	73	SCC	Right	103	T4N2M1a	T4N2M1a	T4N2M1a	4A	4A	4A
20	E	72	SCC	Right	55	T3N0M0	T3N0M0	T3N0M0	2B	2B	2B
21	E	79	SCC	Left	26	T2aNOMO	T2aN0M0	T2aN0M0	1B	1B	1B
22	E	72	SCC	Left	46	T2bN3M1b	T2bN3M1b	T2bN3M1b	4A	4A	4A
23	E	74	SCC	Left	44	T2bN2M1c	T2bN2M1c	T2bN2M1c	4B	4B	4B
24	E	56	SCC	Right	26	T2N3M1c	T4N3M1c	T4N3M1c	4B	4B	4B
25	E	66	SCC	Right	42	T3N0M0	T3N0M0	T3N0M0	2B	2B	2B
26	E	56	SCC	Right	47	T3N3M1c	T3N3M1c	T3N3M1c	4B	4B	4B
27	E	71	SCC	Right	65	T4N3M0	T4N3M0	T4N3M0	3C	3C	3C
28	E	74	SCC	Left	80	T4N3M1c	T4N3M1c	T4N3M1c	4B	4B	4B
29	E	56	SCC	Right	87	T4N2MO	T4N0M0	T4N0M0	3B	3A[d]	3A

True: staging performed with combining histopathologic and imaging findings.
ADC, adenocarcinoma; ^{18}FFDG, ^{18}F–fluorodeoxyglucose; SCC, squamous cell carcinoma; TNM, tumor–node–metastasis.
[a]N2 lymph node calcified on FAPI.
[b]Upstaged on FAPI with pleural involvement.
[c]Anthracotic lymph node on FDG is downstaged on FAPI.
[d]Lymph node on FDG is downstaged on FAPI.

SUV_{max} values in pleural and lung metastases. Similar to our findings, Ballal *et al.* [14] did not observe a difference in SUV_{max} of pleural lesions between FAPI PET/CT and ^{18}F-FDG PET/CT. In our study, ^{68}Ga-FAPI-04 PET/CT changed the M stage in one patient (3.4%). In their study, Li *et al.* [10] reported stage change in 17.6% of patients with FAPI. In our study, the change in disease stage with ^{68}Ga-FAPI-04 PET/CT (three patients, 10.3%) was observed to be lower when compared to the literature. We think that our lower rate of stage change with FAPI might be due to the fact that the majority of patients in our series were extensively metastatic patients.

In their study with 30 adenocarcinoma and 17 SCC patients, Wei *et al.* [13] reported no significant difference in primary tumor FAPI SUV_{max} values between the SCC and adenocarcinoma groups. However, the authors observed significantly higher SUV_{max} in the lymph node and bone metastases of the patients with SCC than adenocarcinoma. In concordance with the literature, we also observed no statistically significant difference in the SUV_{max} and TBR values of primary lesions with adenocarcinoma and SCC pathology on ^{68}Ga-FAPI PET/CT. However, the TBR values of bone metastases were significantly higher in the SCC group than the adenocarcinoma group.

Our study has certain limitations. These include the retrospective nature of the study, limited number of patients, including only adenocarcinoma and SCC subtypes, uneven number of patients in the subgroups, and not being able to compare the imaging results with surgical findings.

Table 5 Comparison of adenocarcinoma and squamous cell carcinoma

	ADC			SCC			
Variables	*N*	Median	Min-max	*N*	Median	Min-max	*P*[a]
Age	9	58	47–72	20	71.5	46–84	0.047
Primary tumor size	9	43	9.8-02	20	65.5	26–103	0.077
Primary tumor FDG SUV	9	7.4	6.4–16.7	20	17.25	1.33–32.6	0.012
Primary tumor FAPI SUV	9	8.7	5–21.3	20	17	0.7–25.8	0.073
Primary tumor FDG TBR	9	13.21	10.78–47.71	20	31.47	5.32–95.88	0.048
Primary tumor FAPI TBR	9	14	7.35–42.7	20	25.50	1.89–50.59	0.09
Bone metastases FDG SUV_{max}	72	5.75	2.4–25.1	46	6.65	2.4–20.6	0.172
Bone metastases FAPI SUV_{max}	84	10.00	3.2–23.6	51	8.40	2.7–33.3	0.744
Bone metastases FDG TBR_{max}	72	2.44	1.09–20.92	46	2.17	0.71–10.88	0.566
Bone metastases FAPI TBR	84	16.31	5.83–33.71	51	10.63	2.33–46.80	0.023
Liver metastases FDG SUV_{max}	11	5.50	3.80–6.60	7	5.80	4.40–16.00	0.425
Liver metastases FAPI SUV_{max}	11	6.10	3.70–7.00	8	6.35	2.80–14.20	0.778
Liver metastases FDG TBR_{max}	11	2.41	1.30–3.00	7	2.25	1.43–4.57	0.860
Liver metastases FAPI TBR	11	5.55	3.36–6.36	8	5.20	0.97–15.78	0.840
Lymph nodes size (mm)	25	12.00	6–25	120	11.00	4–36	0.451
Lymph nodes FDG SUV_{max}	39	7.30	2.2–12.3	115	7.40	1.8–19.1	0.672
Lymph nodes FAPI SUV_{max}	43	14.10	3.3–28.0	117	10.70	1.6–23.5	0.070
Lymph nodes FDG TBR_{max}	39	3.11	0.97–6.83	115	3.82	0.94–12.82	0.178
Lymph nodes FAPI TBR	43	6.55	1.61–12.73	117	6.43	0.84–18.75	0.755

ADC, adenocarcinoma; FAPI, fibroblast activator protein inhibitor; min, minimum; max, maximum; SCC, squamous cell carcinoma; SUV, standardized uptake value; TBR, tumor to background ratio.
[a]Mann–Whitney U test.

Conclusion

Although ^{68}Ga-FAPI-04 PET/CT detected more lesions and higher diagnostic accuracy than ^{18}F-FDG PET/CT in NSCLC, neither method was statistically superior to each other in terms of diagnostic accuracy in TNM staging. Prospective studies with larger patient series are needed in this regard.

Acknowledgements

Conflicts of interest

There are no conflicts of interest.

References

1 Sung H, Ferlay J, Siegel RL, Laversanne M, Soerjomataram I, Jemal A, Bray F. Global cancer statistics 2020: GLOBOCAN estimates of incidence and mortality worldwide for 36 cancers in 185 countries. *CA Cancer J Clin* 2021; **71**:209–249.

2 Siegel R, Ma J, Zou Z, Jemal A. Cancer statistics, 2014. *CA Cancer J Clin* 2014; **64**:9–29.

3 Kalemkerian GP, Loo BW, Akerley W, Attia A, Bassetti M, Boumber Y, *et al*. NCCN Guidelines insights: small cell lung cancer, version 2.2018. *J Natl Compr Canc Netw* 2018; **16**:1171–1182.

4 Maziak DE, Darling GE, Inculet RI, Gulenchyn KY, Driedger AA, Ung YC, *et al*. Positron emission tomography in staging early lung cancer: a randomized trial. *Ann Intern Med* 2009; **151**:221–8, W.

5 Çermik TF, Ergül N, Yılmaz B, Mercanoğlu G. Tumor imaging with 68Ga-DOTA-FAPI-04 PET/CT: comparison with 18F-FDG PET/CT in 22 different cancer types. *Clin Nucl Med* 2022; **47**:e333–e339.

6 Kratochwil C, Flechsig P, Lindner T, Abderrahim L, Altmann A, Mier W, *et al*. 68Ga-FAPI PET/CT: tracer uptake in 28 different kinds of cancer. *J Nucl Med* 2019; **60**:801–805.

7 Chen H, Zhao L, Ruan D, Pang Y, Hao B, Dai Y, *et al*. Usefulness of [68Ga]Ga-DOTA-FAPI-04 PET/CT in patients presenting with inconclusive [18F]FDG PET/CT findings. *Eur J Nucl Med Mol Imaging* 2021; **48**:73–86.

8 Herbst RS, Morgensztern D, Boshoff C. The biology and management of non-small cell lung cancer. *Nature* 2018; **553**:446–454.

9 Ettinger DS, Wood DE, Aisner DL, Akerley W, Bauman J, Chirieac LR, *et al*. Non-small cell lung cancer, version 5.2017, NCCN clinical practice guidelines in oncology. *J Natl Compr Canc Netw* 2017; **15**:504–535.

10 Li Y, Lin X, Li Y, Lv J, Hou P, Liu S, *et al*. Clinical utility of F-18 labeled fibroblast activation protein inhibitor (FAPI) for primary jtaging in lung sdenocarcinoma: a Prospective Study. *Mol Imaging Biol* 2022; **24**:309–320.

11 Wang L, Tang G, Hu K, Liu X, Zhou W, Li H, *et al*. Comparison of 68Ga-FAPI and 18F-FDG PET/CT in the evaluation of advanced lung cancer. *Radiology* 2022; **303**:191–199.

12 Giesel FL, Adeberg S, Syed M, Lindner T, Jiménez-Franco LD, Mavriopoulou E, *et al*. FAPI-74 PET/CT using either 18F-AlF or cold-Kit 68Ga labeling: biodistribution, radiation dosimetry, and tumor delineation in lung cancer patients. *J Nucl Med* 2021; **62**:201–207.

13 Wei Y, Cheng K, Fu Z, Zheng J, Mu Z, Zhao C, *et al*. [18F]AlF-NOTA-FAPI-04 PET/CT uptake in metastatic lesions on PET/CT imaging might distinguish different pathological types of lung cancer. *Eur J Nucl Med Mol Imaging* 2022; **49**:1671–1681.

14 Ballal S, Yadav MP, Moon ES, Kramer VS, Roesch F, Kumari S, *et al*. Biodistribution, pharmacokinetics, dosimetry of [68Ga]Ga-DOTA.SA.FAPi, and the head-to-head comparison with [18F]F-FDG PET/CT in patients with various cancers. *Eur J Nucl Med Mol Imaging* 2021; **48**:1915–1931.

15 Wu Y, Li P, Zhang H, Shi Y, Wu H, Zhang J, *et al*. Diagnostic value of fluorine 18 fluorodeoxyglucose positron emission tomography/computed tomography for the detection of metastases in non-small-cell lung cancer patients. *Int J Cancer* 2013; **132**:E37–E47.

16 Konishi J, Yamazaki K, Tsukamoto E, Tamaki N, Onodera Y, Otake T, *et al*. Mediastinal lymph node staging by FDG-PET in patients with non-small cell lung cancer: analysis of false-positive FDG-PET findings. *Respiration* 2003; **70**:500–506.

17 Betancourt-Cuellar SL, Carter BW, Palacio D, Erasmus JJ. Pitfalls and limitations in non-small cell lung cancer staging. *Semin Roentgenol* 2015; **50**:175–182.

18 Wang J, Welch K, Wang L, Kong FM. Negative predictive value of positron emission tomography and computed tomography for stage T1-2N0 non-small-cell lung cancer: a meta-analysis. *Clin Lung Cancer* 2012; **13**:81–89.

19 Tang W, Wu J, Yang S, Wang Q, Chen Y. Organizing pneumonia with intense 68Ga-FAPI uptake mimicking lung cancer on 68Ga-FAPI PET/CT. *Clin Nucl Med* 2022; **47**:223–225.

20 Shang Q, Zhao L, Pang Y, Meng T, Chen H. Differentiation of reactive lymph nodes and tumor metastatic lymph nodes with 68Ga-FAPI PET/CT in a patient with squamous cell lung cancer. *Clin Nucl Med* 2022; **47**:458–461.

21 Schmidt-Hansen M, Baldwin DR, Hasler E, *et al*. PET-CT for assessing mediastinal lymph node involvement in patients with suspected resectable non-small cell lung cancer. *Cochrane Database Syst Rev* 2014; **2014**:CD009519.

22 Erasmus JJ, Macapinlac HA, Swisher SG. Positron emission tomography imaging in nonsmall-cell lung cancer. *Cancer* 2007; **110**:2155–2168.

23 Li Y, Jin G, Su D. Comparison of gadolinium-enhanced MRI and 18FDG PET/PET-CT for the diagnosis of brain metastases in lung cancer patients: a meta-analysis of 5 prospective studies. *Oncotarget* 2017; **8**:35743–35749.